IET Image Processing

Research Article

IET Journals
The Institution of Engineering and Technology

Novel approach for automatic mid-diastole frame detection in 2D echocardiography sequences for performing planimetry of the mitral valve orifice

ISSN 1751-9659
Received on 30th December 2019
Revised 27th March 2020
Accepted on 12th May 2020
E-First on 8th September 2020
doi: 10.1049/iet-ipr.2019.1757
www.ietdl.org

Mahtab Faraji[1], Hamid Behnam[1] ✉, Mohammad Norizadeh Cherloo[1], Maryam Shojaeifard[2]

[1]Iran University of Science and Technology, Narmak, Tehran, Iran

[2]Rajaei Cardiovascular Medical and Research Center, Tehran, Iran

✉ *E-mail: Behnam@iust.ac.ir*

Abstract: The mitral valve orifice area is a reliable measure for evaluating mitral valve stenosis (MS) severity, which is obtained by the planimetry of the mid-diastole frame in the echocardiography sequences. Since the manual method for determining this frame is time-consuming and user-dependent, a novel automatic method has been proposed in this study. First, the region of interest (ROI) containing the mitral valve orifice region is detected using circular Hough transform and k-means algorithms. Then, the dimension reduction method is applied to the ROI of each frame to map it into a point in a 2D space. The performance of the local linear embedding (LLE), isometric mapping, kernel principal component analysis (PCA), and linear PCA algorithms has been evaluated in this study. Finally, a distance curve is obtained by calculating the Euclidean distance between consecutive points in 2D space, and the mid-diastole frame is determined by interpreting this curve. The proposed algorithm was validated using 2D echocardiography of the 20 MS patients. Finally, the LLE method showed the best result, and the average frame difference for 20 cases using the proposed method compared with the gold standard (the echo-cardiologist opinion) was 1.40.

1 Introduction

Mitral valve stenosis (MS) is a form of valvular heart disease in which the primary cause of this disease in adult patients (<90%) is rheumatoid diseases. However, rheumatic MS is less common in the United States (<1% of the population), but commonly seen in developing countries [1]. In the normal cardiac physiology, the mitral valve opens during the left ventricle diastole to allow blood to flow from the left atrium to the left ventricle. This forward flow direction continues until the pressure in the left atrium is higher than the left ventricle. However, the mitral stenosis causes a mechanical restriction in blood flow from the left atrium to the left ventricle, which is due to the thickening and immobility of the mitral leaflets, the fusion of the chordae tendineae, and calcification of commissural [2]. The main factors for analysing the severity of MS include the calculation of the mitral valve orifice area by the pressure half-time method and also by direct planimetry of the mitral valve orifice, the mean pressure gradient across the mitral valve, and the pressure of the pulmonary artery [2]. According to these factors, mitral valve stenosis is categorised into three grades of mild, moderate, and severe [2]. The mitral valve orifice area can be calculated easily by the pressure half-time method. However, it may be affected by hemodynamic factors such as heart rate, cardiac rhythm, and cardiac index. The direct planimetry of the mitral valve orifice leads to the hemodynamic-independent assessment of mitral valve area [3] and plays the central role in a proper diagnosis or treatment planning of MS. In the mild and moderate MS, certain drugs can reduce symptoms of diseases by easing the heart's workload and regulating its rhythm. In the severe MS, the valve repair or replacement to treat the mitral stenosis is done, which may include surgical (mitral valve replacement) and nonsurgical (percutaneous balloon mitral Valvuloplasty) options [4].

The quantification of the left ventricle function markers such as ejection fraction and global longitudinal strain can be done using the 2D echocardiography. Such echocardiographic measurements usually relate to time points such as end-diastole and end-systole and, therefore, the detection of the end of the left ventricular systole and diastole is necessary. However, in the mitral valve stenosis diagnosis, the calculation of the mitral valve orifice area by the planimetry has an important role, which is done in the mid-diastole frame in the parasternal short axis (PSAX) view of the 2D echocardiography sequences. In this frame, the mitral valve has the most significant area [5]. Therefore, in practice before performing the planimetry, finding the mid-diastole frame is required [2], which is performed manually by an experienced echo-cardiologist. However, it is time-consuming and depends on the cardiologist's experience. As a simplification diagnosis process, developing a system for automatic determination of the mid-diastole frame is needed, which is addressed by this research for the first time.

Most of the researches on the automatic phase detection field has been focused on finding end-systole and end-diastole frames in 2D echocardiography sequences, and some available resources will be reviewed below.

The authors of [6, 7] recognised the end-systole and end-diastole frames using the high-dimensional data visualisation methods such as dimensionality reduction algorithms, which mapped the high dimensional of echocardiography image to low-dimensional space. The authors of [8–10] carried out the further development of artificial neural networks and machine learning algorithms for determining cardiac phases automatically. The real-time estimation of the cardiac cycle phase was the advantage of the introduced methods of these authors. In [11], the authors evaluated the deep learning algorithms for view recognition and end-systolic and end-diastolic frame detection in 2D echocardiography sequences. They demonstrated the potential of the deep learning algorithms in accomplishing the mentioned tasks. Recently, Dezaki *et al.* [12] developed a deep learning framework consisting of a convolution neural network and recurrent neural network to predict the end-diastole and end-systole frames. Fiorito *et al.* [13] proposed a novel method for detecting cardiac events in echocardiography using deep learning algorithms. 3D convolution neural network was employed to extract spatial-temporal features directly from the input video, and end-diastole and end-systole frames were detected automatically. Narang *et al.* [14] reported of machine learning-based system, featuring automated left ventricle function analysis, where automated end-diastolic and end-systolic

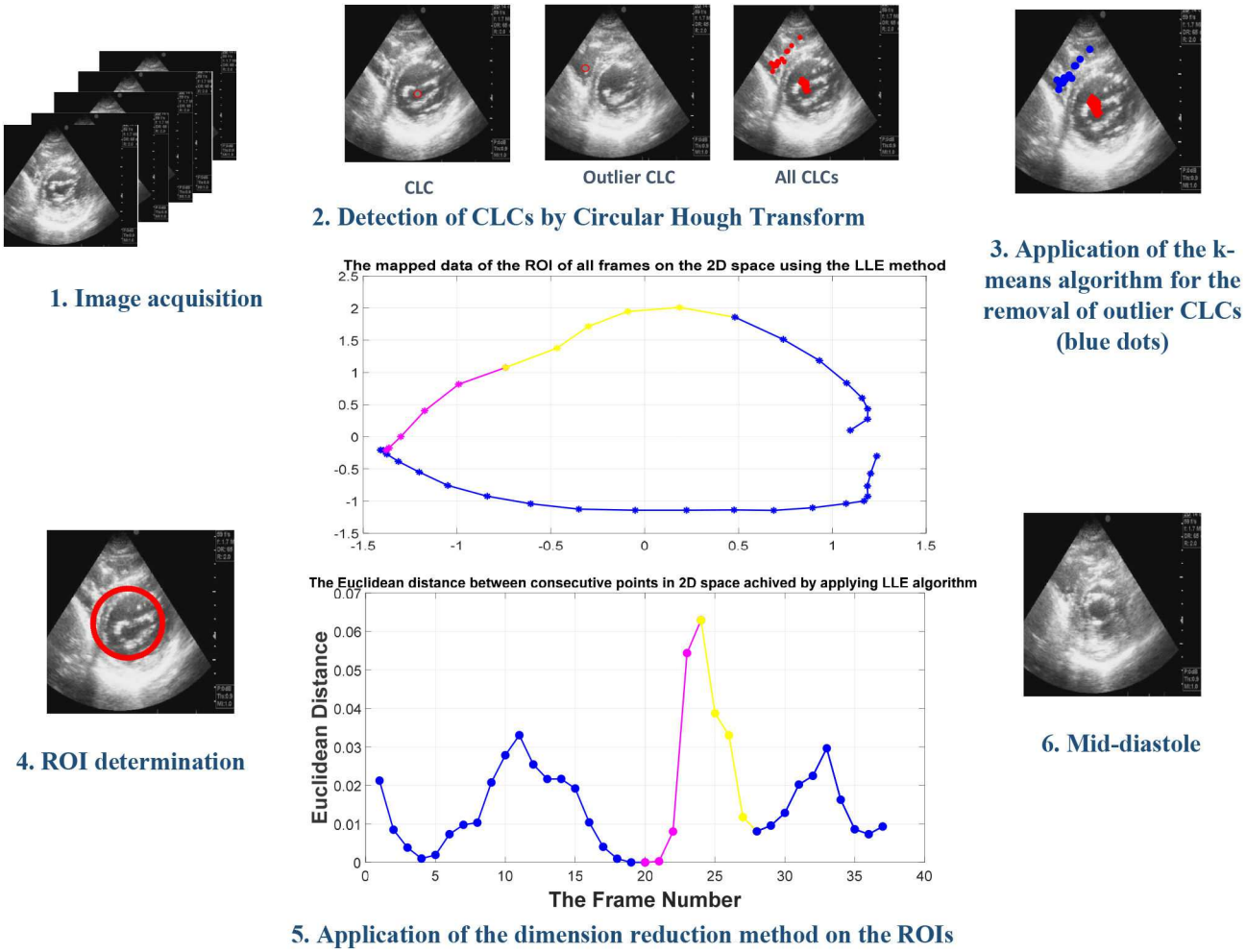

Fig. 1 *Overview of the proposed automatic algorithm for the mid-diastole frame determination. CLC: centre of the largest circle*

frame selection was a part of their study. Recently, another machine learning-based method to left ventricle function analysis by using cardiovascular magnetic resonance (CMR) images proposed in [15]. Their method allows analysis of potentially useful indices of left ventricle ejection/filling parameters. A recent study by Zolgharni [16] concluded that the speckle tracking by the development toolbox, which relies on the block matching algorithm is an efficient method for end-diastole and end-systole frames determination in 2D echocardiography sequences. One research [17] suggested three methods for estimation of the end-diastole frame. In the first method, intensity variation in the region of interest was considered, and the second method was based on the left ventricle deformations in a heart cycle. Finally, the combination of the two previous methods was examined. Some algorithms used segmentation methods for end-systolic and end-diastole frame detection [18]. In the segmentation-based approaches, end-diastole and end-systolic frames are characterised by the assumption that the most significant and smallest left ventricle segmented cross-sections in a cardiac cycle correspond to the end-systole and end-diastole frames. In clinical practice, the end-diastolic and end-systolic frames are manually determined by using the R-wave and T-wave detection in the ECG signal, respectively [16]. The detection of the R-peaks localisation in the noisy signal by using the Hilbert transform combined with a threshold technique was proposed in [19]. As the ECG sampling rate and resolution decreased, their method demonstrated poor performance. Also, a framework to detect aortic valve opening phase with the help of a seismocardiogram (SCG) signal was proposed in [20], which was another study in the automatic cardiac phase-detection field.

Thus, based on the above literature review, to our knowledge, no study has been conducted for finding the mid-diastole frame automatically, which is the first step to perform the planimetry of mitral valve orifice, and previous studies have been focused on finding the end-systole, and end-diastole frames and other cardiac phases.

In this research, a novel automatic method is proposed to the mid-diastole frame detection, which is combined the circular Hough transform algorithm and the dimension reduction method. Circular Hough transform method was employed for the automatic detection of the region of interest (ROI), in which this region was used instead of the whole image in this study. To visualisations of the high-dimensional data of the mitral valve orifice region in all frames, the mapping of this region data into a 2D space was done by the dimension reduction method. Since the mapping quality of the local linear embedding (LLE), isometric mapping (IsoMap), and kernel principal component analysis (PCA) dimensionality reduction methods depend on their free parameters, the residual variance measure has been used to determine their optimal free parameter value.

This paper is divided into five sections. Following the above introduction, Section 2 presents the automatic ROI detection method, as well as the proposed algorithm for determining the mid-diastole frame. Section 3 shows the conducted experiments on mitral valve stenosis cases by four different dimension reduction procedures. Section 4 discusses the obtained results of this work. Finally, the conclusion of this study is given in Section 5.

2 Methods

2.1 Overview

Fig. 1 shows the schematic of the proposed approach for the automatic determination of the mid-diastole frame, which right after image acquisition, the centre of the largest circle (CLC) is determined by applying the circular Hough transform algorithm. Unfortunately, the circular Hough transform may lead to the incorrect definition of the CLC in some frames, and because that

Fig. 2 *Position of the left ventricle cavity and the mitral valve orifice in the parasternal short axis view of 2D echocardiography*

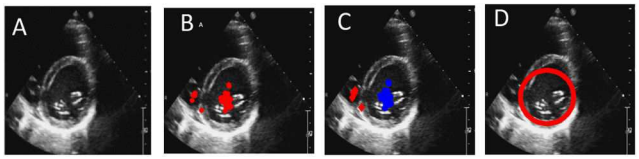

Fig. 3 *Steps to achieve the ROI automatically*
(a) Original frame, ***(b)*** CLC is obtained from all frames by circular Hough transform algorithm (red dot), ***(c)*** Classification of CLCs by *k*-means algorithm and eliminating outliers (red dots), ***(d)*** ROI

the average of CLCs is considered as the final region of interest centre, removing such untrue CLCs is necessary which is done by the unsupervised k-means algorithm in this study. After applying the k-means algorithm on all CLCs, the cluster, which has a smaller number of samples, is regarded as an outlier cluster, and its samples are removed. Therefore, the average position of the remaining CLCs and the radius of the largest circle are considered as centre and radius of the ROI, respectively. Since the variation of the ROI position in the echocardiography sequences is almost negligible, the detected centre and radius can be used for the ROI definition in all frames. Finally, the dimension reduction algorithm is applied to the automatic detected ROI in all frames, and the mapping of data is obtained from high-dimensional space on a 2D space. The distance curve is achieved by calculation of the Euclidean distance between consecutive points in 2D space, and by analysing the distance curve, ECG signal, and echo-cardiologist opinion, the mid-diastole frame is determined. To further evaluation of the proposed method, other distance measures such as Canberra distance, cosine coefficients, and generalised Dice coefficients are also examined [21]. Moreover, the optimal free parameters value for dimension reduction methods is achieved by residual variance measure in this study.

2.2 Image acquisition

There were 20 participants in this study who provided informed consent about involving in this research. The data was collected from the Rajaei Cardiovascular, Medical and Research Center. The Vivid 7 (GE Medical Systems, Horton, Norway) and Affiniti70 (Philips Medical System, US) ultrasound systems were used for recording the data, which six of the echocardiography sequences were obtained with the Affiniti70 and the rest with Vivid 7. Transthoracic 2D echocardiography sequences in PSAX view were acquired, and detection of the mid-diastole frame was performed manually by the experienced echo-cardiologist for evaluating the automatic proposed method.

2.3 CLC detection by circular Hough transform algorithm

One of the popular methods for determining circular objects in image processing is the circular Hough transform algorithm. In [22], a circular Hough transform is used to automatic left ventricle centre point location in the echocardiography sequences in two different levels of the left ventricle in the parasternal short-axis view. By taking into consideration, the position of the mitral valve in parasternal short-axis view in 2D echocardiography sequences, which is located in the left ventricle (Fig. 2), the left ventricle centre point determination by using the circular Hough transform algorithm leads to discovering the approximated mitral valve orifice region centre. The discovered centre point is considered as the CLC in each frame in this study.

According to the circular Hough transform formulation [23], the characteristic equation of a circle of radius $r \in [r_{\min} r_{\max}]$ and centre (a, b) is given by the following equation:

$$(x-a)^2 + (y-b)^2 = r^2 \tag{1}$$

The two following equations can describe this circle:

$$\begin{aligned} x &= a + r\cos(\theta) \\ y &= b + r\sin(\theta) \end{aligned} \tag{2}$$

where (x, y) is the location of the pixel on the circle. Thus, the role of the circular Hough transform is to search for the triplet of parameters (a, b, r). If we know the radius of the circle to be detected in the image, the parameter to search is reduced to a pair (a, b). In echocardiography sequences, the radius range of the left ventricle is based on the geometry of the acoustic window [24], and in the dataset used in this study, $r \in [10\ 100]$ was obtained empirically.

2.4 Removing outlier centres by k-means algorithm and ROI determination

Fig. 3*b* shows the found CLCs in all frames of an echocardiography video in a frame (the red dots). According to this figure, some of the CLCs are far from the focusing region of other centres, which named 'outlier' CLCs.

Since the average position of CLCs has been considered as the ROI centre in this research, outliers may lead to the wrong definition of the ROI. So, discovering outliers and eliminating them is necessary. The outlier removal methods are usually based on distance and clustering methods, in which the k-means algorithm is one of the popular unsupervised clustering ones [25]. The letter k in this algorithm is the number of clusters (in this study, $k = 2$). First, randomly k centre points are assigned, and the distance computes between each sample and all centres, then the sample is attached to the cluster corresponding to the centre having the minimum distance to this sample. Finally, after assigning all samples to the clusters, a new centre point for every cluster is calculated by averaging all samples belonging to the cluster. These processes continue until there is no change in the centre's location. Fig. 3*c* shows the results of CLCs classification using the *k*-means algorithm. Briefly, after applying the *k*-means algorithm, a cluster with a smaller number of CLCs was considered as an outlier cluster, and the corresponding CLCs were removed (red dots in Fig. 3*c*). The average position of the remaining CLCs (blue dots in Fig. 3*c*) and the radius of the largest circle detected in all frames were used as the centre and the radius of the ROI, respectively (Fig. 3*d*).

2.5 Proposed algorithm for automatic mid-diastole frame determination

Dimension reduction tools can be useful for visualisation of data in high-dimensional space by mapping them in low-dimensional space while the information content of the data is preserved [26]. PCA, multi-dimensional scaling, and Fisher's linear discriminant analysis are instances of linear dimension reduction methods. Also, some of the non-linear dimension reduction methods (or manifold learning) include IsoMap, LLE, and kernel PCA algorithms. The manifold learning is one of the non-linear dimension reduction methods, which attempts to preserve perfectly the relationships between neighbourhoods in the process of dimensionality reduction (the relationship can be based on the distance). These methods are divided into two general categories: local and global. Local approaches (such as LLE) guarantee that the nearby points in the high-dimensional space should be mapped to nearby points in the low-dimensional. While, the global approaches (such as IsoMap and kernel PCA) follow the same goal of local methods, but at the same time, high-dimensional faraway data must be mapped to faraway data in low-dimensional space.

In the echocardiography sequence, each frame contains information in the high-dimensional space equalling to the number of pixels in each frame.

So, interpreting the data of a frame and the relationship between consecutive frames of an echocardiography sequence in high-dimensional space is complicated. For visualising this information, frames mapping from a high-dimensional space to 2D space by dimension reduction techniques are required.

In this study, the determination of the mid-diastole frame was done by mapping the ROI information of all frames into a 2D space using the dimension reduction algorithm, and the performance of LLE, IsoMap, kernel PCA and linear PCA algorithms were evaluated for this purpose. In the following, the theory of the mentioned dimension reduction algorithms is described briefly.

2.5.1 Overview of dimensionality reduction methods:

- *The linear PCA algorithm*: In the PCA algorithm, the linear mapping of the data to a low-dimensional space is performed, in which data variance is maximised in the low-dimensional space [27]. The first step in the PCA algorithm is normalisation. Based on the assumption that the mean of data is zero in the PCA algorithm, all intensity values of each column of $\boldsymbol{A}(x, y)$ matrix (which is the ROI intensity matrix) from the total mean of the same column should be subtracted. The second step is the construction of the covariance matrix of the data, and in the next stage, eigenvectors and eigenvalues of the covariance matrix are calculated by the singular value decomposition (SVD) as follows:

$$\boldsymbol{cv} = \boldsymbol{\lambda v} \tag{3}$$

  The $\boldsymbol{c}$ is the covariance matrix, $\boldsymbol{v}$ and $\boldsymbol{\lambda}$ are eigenvectors and eigenvalues of the covariance matrix, respectively. Finally, for data mapping to 2D space, eigenvectors corresponding to the two largest eigenvalues are selected, and by multiplying $A_{\text{normalised}}(x, y)$ by the desired eigenvectors, mapping of data into 2D space is performed.
- *The kernel PCA algorithm*: The kernel PCA is the generalisation of the linear PCA that, unlike the standard linear PCA, allows nonlinear dimensionality reduction, which is helpful for complex data that cannot be well represented in a linear space [28]. In fact, in the kernel PCA algorithm, the data is projected into the new space by a non-linear kernel function.
- Assume we have a non-linear transformation $\varphi(x_i)$ which transfers data from D-dimensional feature space $(\mathbb{R}^n)$ to a high-dimensional space $\left(\mathbb{R}^f\right)$ being linearly separable in this space. So, each data point $x_i (i = 1, \ldots, N)$ is projected into a point $\varphi(x_i)$. Then the linear PCA procedure in the new space can be performed. One of the commonly used kernels is the Gaussian kernels

$$\text{Gaussian kernel: } \exp\left(-\frac{\| x - y \|^2}{2\sigma^2}\right) \tag{4}$$

  In this work, we have used the Gaussian kernel PCA.
- *The LLE algorithm:* The LLE method is a non-linear dimensionality reduction technique to map high-dimensional observation data onto a new low-dimensional space persevering neighbourhood relationship. So, each input data and its k nearest neighbours lie on a locally-linear patch, and then this patch applies in a low-dimensional space. The summary of the LLE algorithm is as follows:

  (i) The k nearest neighbours are chosen for each point using a distance measure such as the *Euclidean* distance, *Mahalanobis,* or *Pearson coefficients* metrics.
  (ii) A set of weights is computed for the reconstruction of the point by its neighbours, which weights cannot be zero, and the sum of the weights equals to one.
  (iii) The embedding vector is computed using weights defined in the previous step.
- For more details of the LLE algorithm, refer to [29].
- *The IsoMap algorithm*: IsoMap algorithm is a non-linear dimensionality reduction method, which tries to preserve the geodesic distances between data in the lower dimension space. This method is an improvement of the multi-dimensional scaling (MDS) dimension reduction method. IsoMap differs from classical MDS in the initial few steps only. Instead of using the Euclidean metric for dissimilarity, it uses graph distances, which consists of three main stages [30]:

  (i) Creating a neighbourhood graph from the dataset by Euclidean metrics.
  (ii) Using the graph distance to the approximate geodesic distance between all pairs of data.
  (iii) Implementing the MDS algorithm.
- Through mapping with geodesic distances, it nicely approximates the close points as neighbours and far away points as distant.

In the next subsection, a measure is introduced to choose the optimum free parameter value in LLE (k), IsoMap (k), and Gaussian kernel PCA (σ) methods, which have a critical role in mapping quality.

2.5.2 Optimal free parameter choice in dimension reduction methods:

In LLE and IsoMap algorithms, if the number of nearest neighbours is large, it will cause smoothing or deletion of small-scale structures. Conversely, if the neighbourhood is poorly selected, it can mistakenly divide the continuous manifold into discrete manifolds. In the Gaussian kernel PCA, σ is a parameter that controls the width of the Gaussian kernel and the flexibility of the model. In fact, for large values of σ, the data mapping is nearly linear. One of the methods for choosing the optimal free parameter value in the dimension reduction algorithms is to check the mapping quality for different free parameter values. It is necessary to define a measure of information preservation for the dimensionality reduction process, to evaluate the embedding quality of high-dimensional data obtained with the dimension reduction method. The residual variance is commonly used to evaluate how well the pairwise distances are preserved and is used to determine the optimal free parameter value in dimension reduction methods. It is a quantitative criterion for estimating the quality of input–output mapping and showing how high-dimensional data is mapped to low-dimensional space. This metric is defined as follows:

$$\xi_{r\,\text{var}} = 1 - \rho^2_{\boldsymbol{D}_x \boldsymbol{D}_y} \tag{5}$$

where ρ is the standard linear correlation coefficient taken over all entries of $\boldsymbol{D}_x$ and $\boldsymbol{D}_y$, $\boldsymbol{D}_x$ and $\boldsymbol{D}_y$ are the matrices of the Euclidean distances between pairs of points in X and Y, respectively. X and Y are the input high-dimensional data set and output embedded low-dimensional data set, respectively[31]. The possible value of residual variance ranges from 0 to 1. Generally, the lower the residual variance indicates the better the high-dimensional data mapping quality in the embedded space.

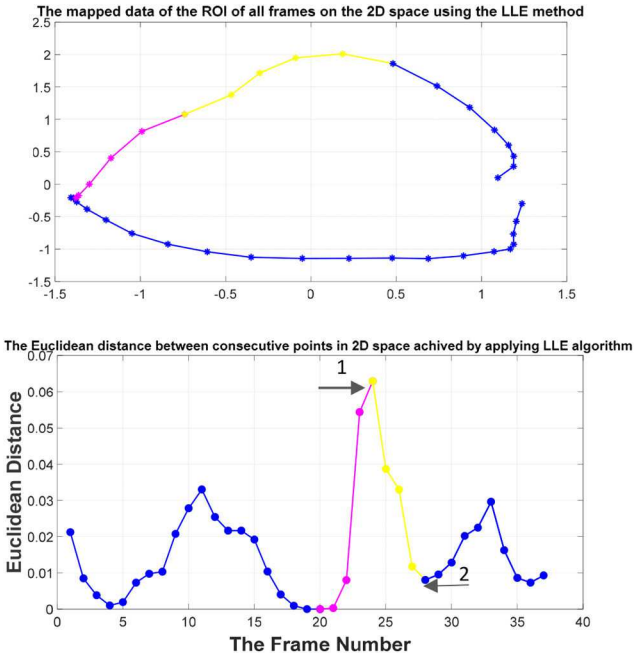

Fig. 4 ***Top****: The mapped data of the ROI of all frames on the 2D space using the LLE method.* ***Bottom:*** *The representation of the Euclidean distance curve between every two consecutive points in the 2D space. Each of the small circles is equivalent to a frame. Parts 1 and 2 correspond to Fig. 5 sections.* ***Purple colour part****: rapid filling phase;* ***yellow colour part****: diastasis phase;* ***blue colour part****: other cardiac phases*

2.5.3 Implementation of dimension reduction for finding the mid-diastole frame: To implement the dimension reduction approaches, including LLE, IsoMap, linear PCA, and kernel PCA algorithms on each case, the ROI of all frames, which achieved automatically in the previous section, was considered. Therefore, in our study, instead of the whole image, a smaller part of the image (ROI) was regarded, most of the valuable information centres in this region. Then, after applying the dimension reduction algorithm with optimal free parameter value (obtained by residual variance measure), the ROI of all frames was mapped to the new 2D space. Subsequently, the distance curve was achieved by computing the Euclidean distance between consecutive points in two-dimensional space and was employed to determine the mid-diastole frame. Fig. 4 displays the mapped data of the ROIs of the echocardiography sequence on the 2D space using the LLE algorithm and the associated Euclidean distance curve for a subject (each of small dots is equivalent to a frame).

The distance curve of Fig. 4 is comparable to the trend of the ventricular volume variation curve in Fig. 5 (in diastole phase). As illustrated in Fig. 5, the ventricle volume increases in the 'rapid inflow' phase because of the mitral valve opening and rapid filling of the left ventricle (purple colour part in Fig. 4). Since in the 'diastasis' phase, the pressure in both the left ventricle and the left atrium is equal, there is an insignificant change in the ventricular volume (yellow colour part in Fig. 4). Then, because of the atrial contraction, the volume of the left ventricle rises [33]. The minima of Fig. 4 are also corresponding to Fig. 5 (parts 1 and 2). Through investigating cardiac frames, ECG signal, their corresponding points in the distance curve and experienced echo-cardiologist diagnosis on 20 different cases, it has been derived that the highest pick (part 1) corresponds to end of the 'rapid inflow', which represents the early-diastole frame and the minimum after that (part 2) shows the end of the 'diastasis' phase, which denotes the mid-diastole frame.

The correct cardiac phase for performing the planimetry of mitral valve orifice is the mid-diastole phase being the most significant opening state of the mitral valve [5]. Fig. 6 shows two frames of the 2D echocardiography sequence in PSAX view at the tips of mitral valve leaflets in early-diastole and mid-diastole phases. In the next section, the performance of different dimension

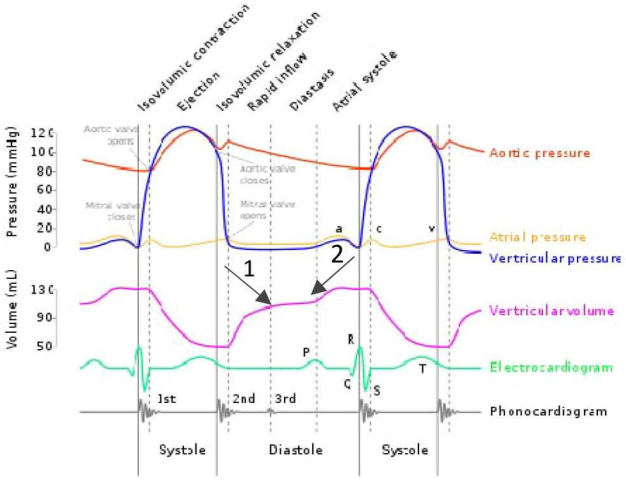

Fig. 5 *Demonstration of different stages of the diastolic cardiac phase. Parts 1 and 2 correspond to the highest peak and the minimum after that in Fig. 4 respectively [32]*

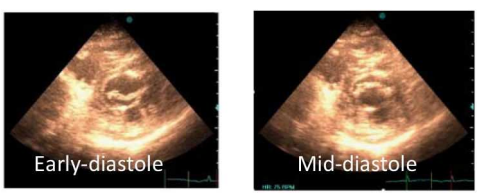

Fig. 6 *Displaying the early-diastole (left) and mid-diastole (right) frames in one subject in 2D echocardiography in PSAX view at the tips of mitral valve leaflets*

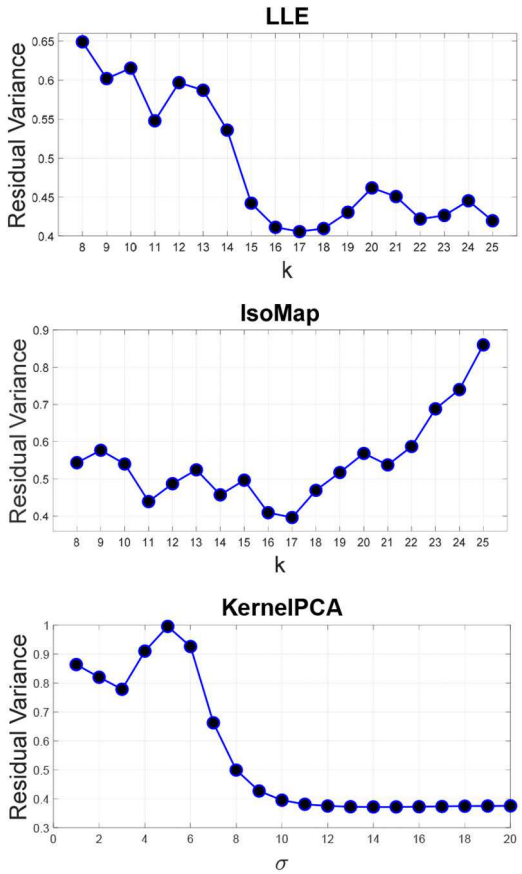

Fig. 7 *Residual variance variation concerning the free parameter of the dimension reduction algorithms (k in LLE and IsoMap, and σ in Gaussian kernel PCA) for one specific case*

Table 1 Optimal neighbouring value in the LLE and IsoMap algorithms, and σ value in kernel PCA method for 20 different cases

Case/method	#1	#2	#3	#4	#5	#6	#7	#8	#9
LLE (k)	17	15	23	13	24	16	16	12	21
IsoMap (k)	11	12	12	22	23	24	24	14	21
kernel PCA (σ)	7	12	12	9	9	19	19	16	19

Case/method	#10	#11	#12	#13	#14	#15	#16	#17	#18	#19	#20
LLE (k)	16	14	18	17	11	11	14	11	11	15	19
IsoMap (k)	18	14	21	16	20	12	11	11	11	13	13
kernel PCA (σ)	19	19	12	10	8	14	10	8	5	6	7

reduction methods to determine the mid-diastole frame automatically will be assessed.

3 Results

3.1 Assessment of free parameter selection in dimension reduction algorithms

In this study, the residual variance measure was employed to discover the appropriate free parameter value of the three mentioned dimension reduction algorithms. The optimal value indicates that with the selected value, the algorithm solves the problem of dimensionality reduction with higher accuracy and obtains meaningful data structures in lower-dimensional space. Fig. 7 illustrates the residual variance variation concerning the free parameter of each mentioned dimension reduction algorithm (k in LLE and IsoMap and σ kernel PCA) for one case. The optimal free parameter value for each algorithm was obtained by applying the algorithm with various free parameter values (in this study, $8 < k < 25$ for both LLE and IsoMap methods, and $1 < \sigma < 20$ for Gaussian kernel width were considered) on the ROI of all frames of the echocardiography sequence. The value which was minimised the residual variance was considered as the optimal free parameter one. The optimal value for the LLE, IsoMap, and kernel PCA algorithms was 17, 17, and 11, respectively. Table 1 shows the calculated optimal neighbouring value in LLE and IsoMap algorithms and σ value in the kernel PCA method for 20 different cases by using the residual variance method. As one can see, the constant optimum value was not obtained for either method. This may be due to the complex structure of the mitral valve in different cases (Fig. 8). So, discovering the optimal value of the dimension reduction algorithm's parameter is critical in this study, which was done by the residual variance measure.

3.2 Comparison of different dimension reduction algorithms for the mid-diastole frame determination

Fig. 9 illustrates the two-dimensional manifolds taken by applying three mentioned dimension reduction methods in achieved optimal free parameter values and for the linear PCA algorithm for the case of Fig. 7. Fig. 9 indicates that the manifold of the LLE, IsoMap, and kernel PCA algorithms provides meaningful structure, while

Fig. 8 *Structure of the mitral valve in the mid-diastole frame in three different cases*

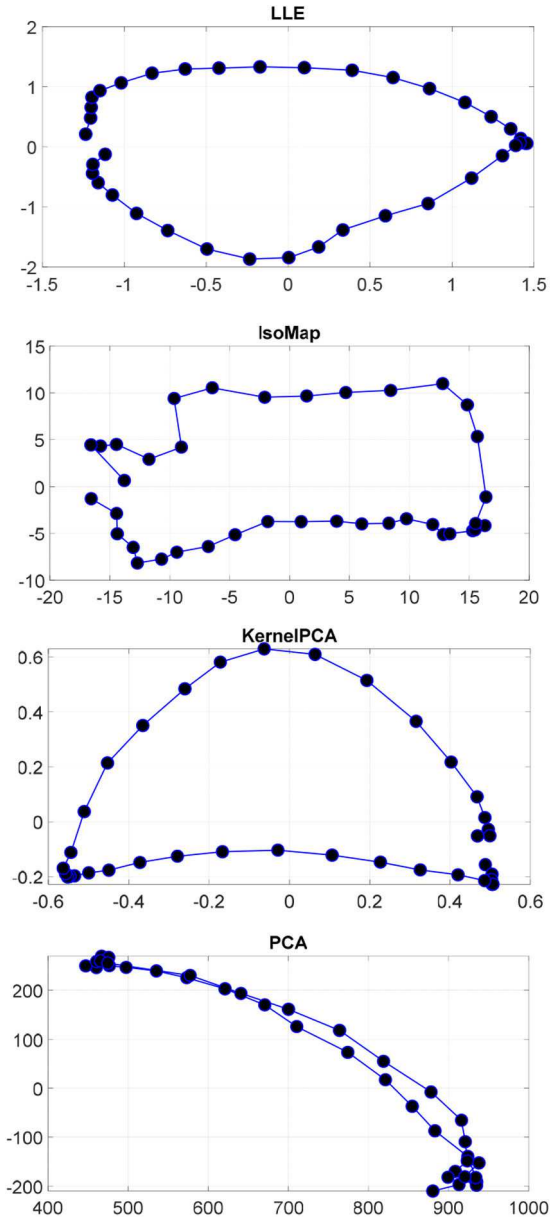

Fig. 9 *Two-dimensional manifolds taken by applying three mentioned dimension reduction methods in determined optimal free parameter values and for the linear PCA algorithm*

the linear PCA algorithm does not cause meaningful ones. According to the disappointing result of the linear PCA mapping to create a meaningful structure in our dataset, the comparison of the LLE, kernel PCA, and IsoMap algorithms was examined to discover the mid-diastole frame. Fig. 10 shows the obtained Euclidean distance curves by applying three the dimension reduction methods, including LLE, IsoMap, and Kernel PCA algorithms, on the two different cases (the cyan circle is the detected mid-diastole frame automatically, and the red diamond is the experienced echo-cardiologist diagnosis). In case #1, the frame difference error in the LLE, IsoMap, and kernel PCA is 0, 1, 1, respectively, while in case #2 equals to 1 in all three methods. The performance of the three approaches in case #2 was identical, but in case #1, the LLE method produced a better outcome than the other two methods.

Table 2 presents the result of applying the proposed automatic mid-diastole frame detection method in twenty cases. It is clear that the LLE was more successful than the other two methods, and the average frame difference achieved by the comparison of the automatic method result and the manual diagnosis performed by the expert echo-cardiologist was 1.4, while in IsoMap and kernel PCA algorithm was 2.05 and 2.2, respectively. Also, the maximum frame difference error achieved by applying LLE, IsoMap, and kernel PCA algorithms was 3, 4, and 5 frames, respectively.

As you can see, by considering the Euclidean distance measure to discover the mid-diastole frame, the LLE algorithm performs better than the other two dimension reduction methods. To confirm the applicability of the LLE method, the impact of the other distance measures such as the Canberra distance, cosine coefficients, and generalised dice-coefficients were examined on

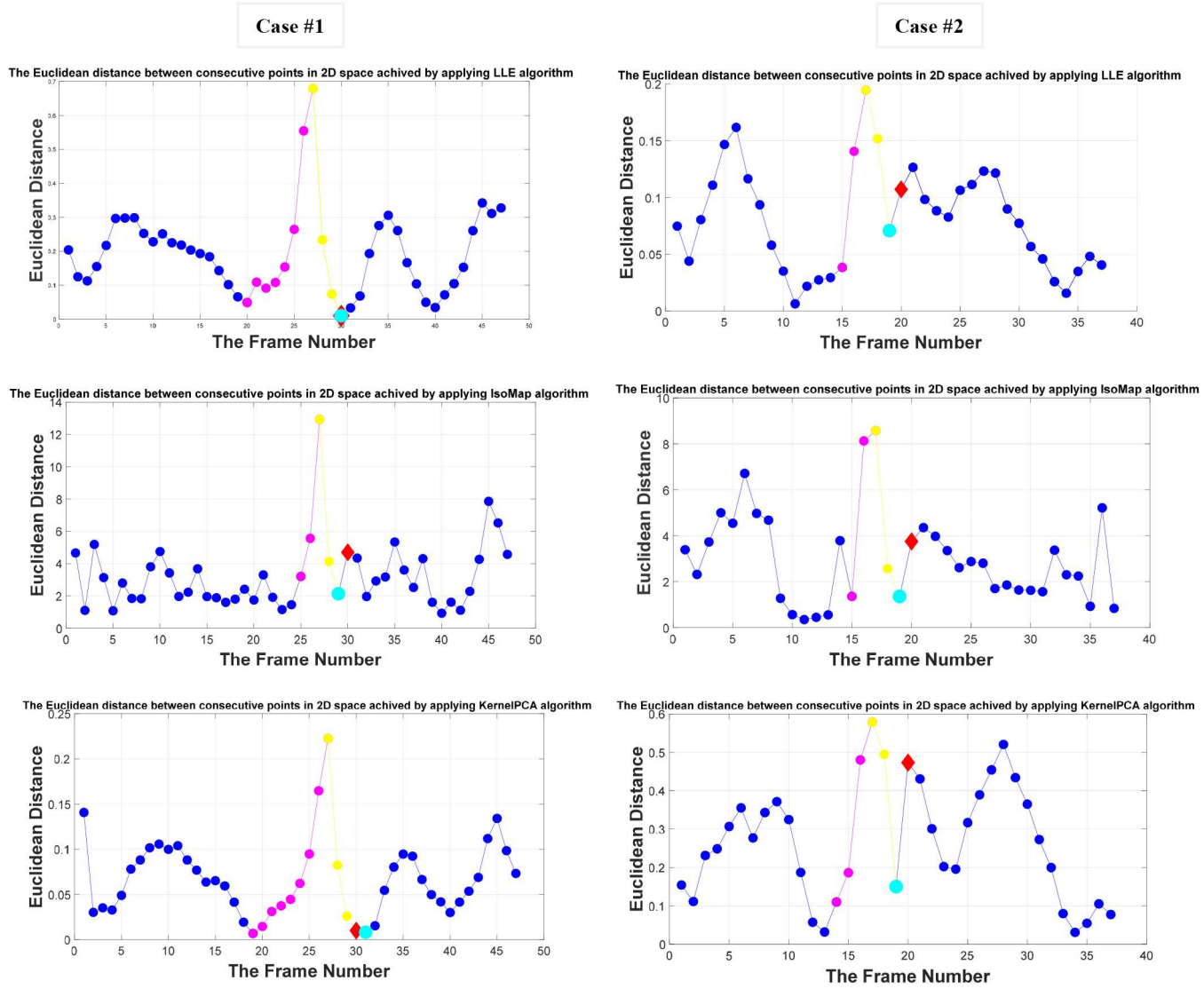

Fig. 10 *Obtained Euclidean distance curves by employing the LLE (first row), IsoMap (second row), and kernel PCA (third row) algorithms, on two cases.* ***Cyan circle****: the detected mid-diastole frame automatically;* ***red diamond****: the experienced echo-cardiologist diagnosis;* ***purple colour part****: rapid filling phase;* ***yellow colour part****: diastasis phase;* ***blue colour part****: other cardiac phases. Each of small circles is equivalent to a frame*

Table 2 Comparison of the LLE, IsoMap, and kernel PCA algorithms for finding the mid-diastole frame in 20 different cases. The last column represents the average frame difference, and the numerical values in other columns show the frame difference

Case/method	#1	#2	#3	#4	#5	#6	#7	#8	#9	#10	#11	#12	#13	#14	#15	#16	#17	#18	#19	#20	Average frame difference
LLE (k)	1	2	0	1	1	1	1	3	3	1	3	2	2	1	1	1	1	0	3	0	**28/20 = 1.40**
IsoMap (k)	3	2	3	2	1	1	1	4	0	1	4	0	2	3	4	3	1	4	0	2	**41/20 = 2.05**
kernel PCA (σ)	2	2	3	1	0	1	1	2	0	4	3	3	5	5	3	3	3	1	0	1	**44/20 = 2.20**

Table 3 Comparison of the Euclidean distance, the Canberra distance, cosine coefficients, and generalised dice coefficients for the mid-diastole frame detection

Measure/method	Euclidean	Canberra	Cosine coefficients	Generalised dice coefficients
LLE	**1.40**	2.40	2.50	1.95

the mid-diastole frame discovery. Table 3 displays the average frame difference results of the different distance indicators for mid-diastole frame determination by employing the LLE algorithm. As shown in the table, all distance measures are successful in mid-diastole frame detection. However, the Euclidean distance performed a little better than the other similarity measures.

3.3 Investigating the effects of using the mitral valve orifice region

In this section, the result of using the ROI instead of the whole frame in mid-diastole frame determination is presented. Fig. 11 shows the accuracy of the LLE algorithm for both using the entire image (left column) and only the ROI (right column) for two different cases. It is clear that by using the whole frame, the obtained frame difference in case #1 was significant (equal to five frames) while considering only the ROI, the obtained result was following the echo-cardiologist diagnosis. Also, in case #2, when using the whole frame, the uninterpretable result was achieved, but the frame difference error was equal to one by using the ROI. In this study, experiments were run in 2017B software, on an Intel Core (TM) i7–8700 K CPU running at 3.70 GHz. Since the result of using the whole image in the mid-diastole frame determination was uninterpretable in some cases, comparing the average frame

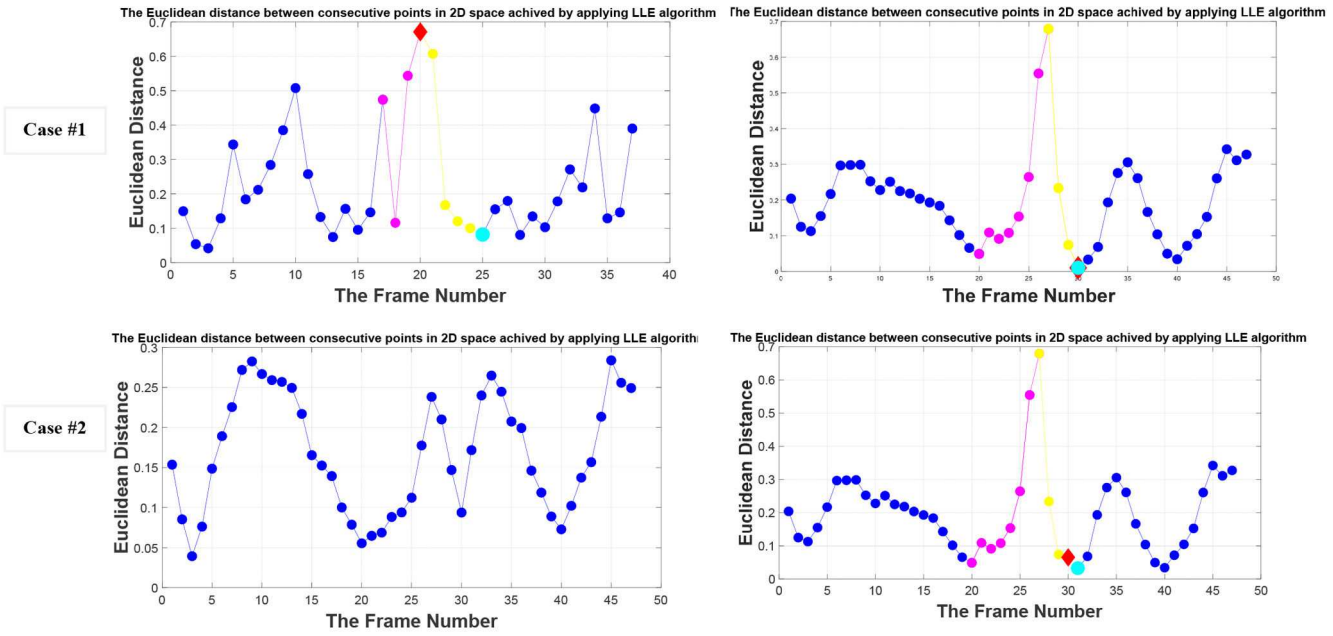

Fig. 11 *Comparison of the result of the mid-diastole frame determination by applying the LLE algorithm for two different cases.* ***Left****: the whole of all frames.* ***Right****: ROI of all frames.* ***Cyan circle****: the detected mid-diastole frame automatically;* ***red diamond****: the experienced echo-cardiologist diagnosis;* ***purple colour part****: rapid filling phase;* ***yellow colour part****: diastasis phase;* ***blue colour part****: other cardiac phases. Each of small circles is equivalent to a frame*

difference in two states (using the whole image and ROI) was not available. However, the average processing time for the whole frame was about 10 min, while the ROI of frames was <1 s. The result proved that using the ROI not only decreases the computational cost but also enhances the accuracy of the proposed method.

4 Discussion

An ECG recording system is a powerful tool in cardiac ultrasound imaging systems, which helps the echo-cardiologist to find the mid-diastole frame. However, the robust detection of this frame is a challenge.

In Fig. 3, 50 frames were taken from an echocardiography sequence for ROI detection by the circular Hough transform algorithm, and 45 of CLCs were located within the ROI and the rest outside it (called outliers). One of the reasons for the occurrence of outlier CLCs is the low quality of the echocardiography sequence, which causes the left ventricle not to be seen well in the image, and the other reason is that, because of the 'fish mouth' shape of mitral valve [2] in diastole phase, circular Hough transforms could not detect the circular shape of the left ventricle. Generally, the circular Hough transform algorithm was successful in the ROI determination in twenty different cases, which showed a high potentiality of this method in detecting this region. Typically, for determining the optimal free parameter value in dimension reduction algorithms, a quantitative measure for a specific range of free parameters should be calculated. So, in [34], Spearman's rho measure was used to find the optimal k value of the LLE algorithm, which estimates the correlation of rank-order data. Also, in [35], a visualisation metric was employed, which was based on the correlation coefficient that was computed the pairwise geodesic distance vector between the original manifold and the lower-dimensional embedding results. Also, automatic tuning of the kernel parameters in the kernel PCA algorithm is necessary, which several researchers proposed algorithms for solving it, especially in the context of the support vector machine (SVM) [36], and kernel parallel analysis (KPA) [37], which had high computational cost. Because the data visualisation problem was raised in this study, we used the same method of finding the optimal k value in the LLE and IsoMap algorithms for the optimal Gaussian kernel width discovering too. So, the residual variance was used to discover the optimal free parameter values, which is another measure for evaluating the mapping quality and has low computational complexity and provides reliable results. From the result of the LLE algorithm in Table 2, we concluded that the LLE algorithm provided the best performance, which has a lower average frame difference. Also, the maximum number of frame differences in the LLE algorithm was lower comparing two other methods. The squared exponential kernel, like the Gaussian kernel, is generally more flexible than the linear or polynomial kernel. Although the results obtained for the kernel PCA method with the Gaussian kernel were comparable to the IsoMap algorithm, the results of the IsoMap algorithm were more accurate. The LLE algorithm gives a better mapping quality than the other mentioned dimension reduction methods, which is maybe because that the LLE method is the local dimension reduction method, and its main focus is to preserve the neighbourhood of similar data in low dimensional space. While the IsoMap and the kernel PCA methods are the global approaches, and all points are examined simultaneously, which may cause errors. Since the linear techniques such as linear PCA algorithm seek to find a linear relationship between data and because of the non-linearity behaviour of data in the real world, this algorithm was not successful in our data. The performance of a distance measure depends on how data distributed on space. Through the investigation of different distance measures, it was obvious that the Euclidean distance performs better than other distance measures. It may be because that the Euclidean distance performs well when deployed to datasets that include compact or isolated clusters. In this paper, two other methods were also evaluated to find the mid-diastole frame. In the first method, after finding the ROI, the intensity variations inside the region of interest are considered to find the desired frame, which did not provide an accurate result. In the second method, we used the segmentation methods to find the mitral valve area, which could use to discover the mid-diastole frame. However, because the mitral valve leaflets do not have a continuous structure in PSAX view in some patients, this method was not suitable. Also, the image processing methods were used to create a continuous structure in the mitral valve leaflets, but these methods changed the area of the mitral valve. Also, the application of artificial intelligence methods to determine the mid-diastole frame is accompanied by serious limitations such as the need for large numbers of data. Therefore, the visualisation of echocardiography sequences by using dimension reduction methods was an appropriate choice to find the mid-diastole frame. As mentioned in the introduction, there have not been any researches that focus on detecting the mid-diastole frame automatically, and in the following section, we consider related works such as the automatic end-systole and end-diastole frame

detection by 2D echocardiography and using ECG sound analysis. For comparison of the proposed method and previous studies, we considered the performance of the three previous kinds of research, which designed to solve the cardiac phase-detection problem. In [18], the authors reported an average of 0.20 and 1.43 frame mismatch for the end-diastole and end-systole frames, respectively. They implemented a deep learning framework, consisting of the CNN and RNN modules to predict the end-diastole and end-systole frames. In another study [13], the 3D CNN model performed for detecting cardiac events on a dataset consisting of standard B-mode images of apical four- and two-chamber views. The mean absolute error was 1.63 and 1.71 frames from end-diastole/end-systole reference, respectively. Deep learning methods have been successful in various applications, and with increasing depth of CNN, classification accuracy increases. However, as pointed out in [38], degradation is one of the issues preventing efficient training of deep models. Compared to previous research [12, 13], we achieved a 1.40 error frame difference by the analysis of echocardiography videos for the detection of the mid-diastole frame. In the previous studies, automatic phase detection was detected based on deep learning method, which requires a huge number of data for training, there are many hyper-parameters to be set by a human (i.e. number of layers, filters, filter shape, etc.), and requires high-performance hardware. On the other hand, the proposed method can reduce the workload of clinicians, and it takes less time to process.

There is a limitation to be addressed in this study. The poor image quality patients precluded mitral orifice area region determination and its appropriate analysis in this study. Although the new-generation ultrasound imaging systems indeed yielded improvements in image quality in a large number of subjects, ∼4% of subjects still had poor image quality [38]. So, the proposed method has a limitation for poor image quality patients.

In addition to mid-diastole frame detection, the proposed algorithm may be used for detection of the most opened mode of the other heart valves, like the mid-systole frame in the aortic valve opening phase (for planimetry in aortic valve stenosis cases) [39].

5 Conclusion

In summary, a novel automatic algorithm for the mid-diastole frame detection in 2D echocardiography sequences in the PSAX view was presented. The automatic detection of the approximated mitral valve orifice region was done by the combination of circular Hough transform and *k*-means algorithms. Also, for the mid-diastole frame determination, four the dimension reduction methods, including the LLE, IsoMap, kernel PCA, and linear PCA, were assessed, but the LLE algorithm presented better results than other dimension reduction methods.

6 References

[1] Tan, T., Hung, J.: 'Standard transthoracic echocardiography and transesophageal echocardiography views of mitral pathology that every surgeon should know', *Ann. Cardiothorac. Surg.*, 2015, **4**, pp. 449–460

[2] Omran, A.S., Arifi, A.A., Mohamed, A.A.: 'Echocardiography in mitral stenosis', *J. Saudi. Heart. Assoc.*, 2011, **23**, (1), pp. 51–58, doi: https://doi.org/10.1016/j.jsha.2010.07.007

[3] de Agustin, J.A., Zamorano, J.L.: 'Valvular heart disease – stenosis', in Buck, T., Franke, A., Monaghan, M.J. (Eds): '*Three-dimensional echocardiography*' (Springer, Berlin, Heidelberg, 2015), pp. 171–193

[4] Nishimura, R., Otto, C.M., Bonow, R.O., *et al.*: '2014 AHA/ACC guideline for the management of patients with valvular heart disease', *J. Am. Coll. Cardiol.*, 2014, **63**, pp. e57–e185, doi: 10.1016/j.jacc.2014.02.536

[5] Saxena, A.: 'Echocardiographic diagnosis of chronic rheumatic valvular lesions', *Glob. Heart.*, 2013, **8**, (3), pp. 203–212, doi: https://doi.org/10.1016/j.gheart.2013.08.007

[6] Gifani, P., Behnam, H., Shalbaf, A., *et al.*: 'Automatic detection of end-diastole and end-systole from echocardiography images using manifold learning', *Physiol. Meas.*, 2010, **31**, pp. 1091–1103, doi: 10.1088/0967-3334/31/9/002

[7] Shalbaf, A., Behnam, H., Gifani, P., *et al.*: 'Automatic detection of end systole and end diastole within a sequence of 2-D echocardiographic images using modified isomap algorithm'. 2011 1st Middle East Conf. on Biomedical Engineering, MECBME 2011, Sharjah, United Arab Emirates, 02/01 2011, doi: 10.1109/MECBME.2011.5752104

[8] Yang, F., He, Y., Hussain, M., *et al.*: 'Convolutional neural network for the detection of End-diastole and End-systole frames in free-breathing cardiac magnetic resonance imaging', *Comput. Math. Methods Med.*, 2017, **2017**, pp. 1–10, doi: 10.1155/2017/1640835

[9] Sundaramurthy, S., Wahi, A., Devi, L. P., *et al.*: 'Cardiac cycle phase detection in echocardiography images using ANN'. 2014 Int. Conf. on Intelligent Computing Applications, Coimbatore, India, 6–7 March 2014, pp. 275–279, doi: 10.1109/ICICA.2014.65

[10] Bibicu, D., Moraru, L.: 'Cardiac cycle phase estimation in 2-D echocardiographic images using an artificial neural network', *IEEE Trans. Biomed. Eng.*, 2013, **60**, (5), pp. 1273–1279, doi: 10.1109/TBME.2012.2231864

[11] Karuzas, A., Sablauskas, K., Skrodenis, L., *et al.*: 'P1465artificial intelligence in echocardiography – steps to automatic cardiac measurements in routine practice', *Eur. Heart J.*, 2019, **40**, (Supplement_1), pp. 773–773, doi: 10.1093/eurheartj/ehz748.0230

[12] Dezaki, F., Liao, Z., Luong, C., *et al.*: 'Cardiac phase detection in echocardiograms with densely gated recurrent neural networks and global extrema loss', *IEEE Trans. Med. Imaging*, 2019, **38**, pp. 1821–1832, doi: 10.1109/TMI.2018.2888807

[13] Fiorito, A.M., Østvik, A., Smistad, E., *et al.*: 'Detection of cardiac events in echocardiography using 3D convolutional recurrent neural networks'. 2018 IEEE Int. Ultrasonics Symp. (IUS), Kobe, Japan, 22–25 October 2018, pp. 1–4, doi: 10.1109/ULTSYM.2018.8580137

[14] Narang, A., Mor-Avi, V., Prado, A., *et al.*: 'Machine learning based automated dynamic quantification of left heart chamber volumes', *Europ. Heart J. - Cardiovascular Imaging*, 2018, **20**, (5), pp. 541–549, doi: 10.1093/ehjci/jey137

[15] Goyal, N., Mor-Avi, V., Volpato, V., *et al.*: 'Machine learning based quantification of ejection and filling parameters by fully automated dynamic measurement of left ventricular volumes from cardiac magnetic resonance images', *Magn. Reson. Imaging*, 2020, **67**, pp. 28–32, doi: https://doi.org/10.1016/j.mri.2019.12.004

[16] Zolgharni, M., Negoita, M., Dhutia, N.M., *et al.*: 'Automatic detection of end-diastolic and end-systolic frames in 2D echocardiography', *Echocardiography*, 2017, **34**, pp. 956–967, doi: 10.1111/echo.13587

[17] Kachenoura, N., Delouche, A., Herment, A., *et al.*: 'Automatic detection of End systole within a sequence of left ventricular echocardiographic images using autocorrelation and mitral valve motion detection'. Proc. of the Annual Int. Conf. of the IEEE Engineering in Medicine and Biology Society, Lyon, France, 2007, vol. 2007, pp. 4504–4507, doi: 10.1109/IEMBS.2007.4353340

[18] Anas, A., Wirza, R., Kadiman, S.: 'Automatic detection of the end-diastolic and end-systolic from 4D echocardiographic images', *J. Comput. Sci.*, 2015, **11**, pp. 230–240, doi: 10.3844/jcssp.2015.230.240

[19] D'Aloia, M., Longo, A., Rizzi, M.: 'Noisy ECG signal analysis for automatic peak detection', *Information*, 2019, **10**, (2), p. 35. Available at https://www.mdpi.com/2078-2489/10/2/35

[20] Choudhary, T., Bhuyan, M.K., Sharma, L.N.: 'A novel method for aortic valve opening phase detection using SCG signal', *IEEE Sens. J.*, 2020, **20**, (2), pp. 899–908, doi: 10.1109/JSEN.2019.2944235

[21] Li, X., Shen, H., Li, H., *et al.*: 'Patch matching-based multitemporal group sparse representation for the missing information reconstruction of remote-sensing images', *IEEE J. Sel. Top. Appl. Earth Obs. Remote Sens.*, 2016, **9**, (8), pp. 3629–3641, doi: 10.1109/JSTARS.2016.2533547

[22] Bansod, P., Desai, U., Burkule, N.: 'Automatic detection of left ventricle in echocardiographic sequences using radial search and temporal smoothing', Cardiff, UK, 2007, pp. 139–142

[23] Cherabit, N., Chelali, F., Djeradi, A.: 'Circular Hough transform for iris localization', *Sci. Technol.*, 2012, **2**, pp. 114–121, doi: 10.5923/j.scit.20120205.02

[24] Göbl, R., Virga, S., Rackerseder, J., *et al.*: 'Acoustic window planning for ultrasound acquisition', *Int. J. Comput. Assist. Radiol. Surg.*, 2017, **12**, pp. 993–1001, doi: 10.1007/s11548-017-1551-3

[25] Kaliyaperumal, S., Kuppusamy, M.: 'Outlier detection in multivariate data', *Appl. Math. Sci.*, 2015, **9**, pp. 2317–2324, doi: 10.12988/ams.2015.53213

[26] Verleysen, M., Lee, J.A.: 'Nonlinear dimensionality reduction for visualization', in, Lee, M., Hirose, A., Hou, Z.-G., Kil, R.M. (Eds): '*Neural information processing*' (Springer, Berlin, Heidelberg, 2013), pp. 617–622

[27] Keerthi Vasan, K., Surendiran, B.: 'Dimensionality reduction using principal component analysis for network intrusion detection', *Perspectives Sci.*, 2016, **8**, (8), pp. 510–512, doi: https://doi.org/10.1016/j.pisc.2016.05.010

[28] Binol, H.: 'Ensemble learning based multiple kernel principal component analysis for dimensionality reduction and classification of hyperspectral imagery', *Math. Probl. Eng.*, 2018, **2018**, pp. 1–14, doi: 10.1155/2018/9632569

[29] Roweis, S.T., Saul, L.K.: 'Nonlinear dimensionality reduction by locally linear embedding', *Science*, 2001, **290**, pp. 2323–2326

[30] Tenenbaum, J., Silva, V., Langford, J.: 'A global geometric framework for nonlinear dimensionality reduction', *Science*, 2001, **290**, pp. 2319–2323, doi: 10.1126/science.290.5500.2319

[31] Alvarez-Meza, A., Valencia-Aguirre, J., Daza-Santacoloma, G., *et al.*: 'Global and local choice of the number of nearest neighbors in locally linear embedding', *Pattern Recognit. Lett.*, 2011, **32**, pp. 2171–2177, doi: 10.1016/j.patrec.2011.05.011

[32] John Hall, A.G.: '*Guyton and hall textbook of medical physiology*' (Elsevier, USA, 2006, 12th Edn.), p. 1120

[33] Nagueh, S.F., Smiseth, O.A., Appleton, C.P., *et al.*: 'Recommendations for the evaluation of left ventricular diastolic function by echocardiography', *J. Am. Soc. Echocardiogr.*, 2009, **22**, (2), pp. 107–133, doi: 10.1016/j.echo.2008.11.023

[34] Kurasova, O., Dzemyda, G.: 'Selection of the number of neighbours of each data point for the locally linear embedding algorithm', *Inf. Technol. Control*, 2007, **36**, pp. 359–364

[35] Tsai, F.S.: 'Comparative study of dimensionality reduction techniques for data visualization', *J. Artif. Intell.*, 2010, **3**, pp. 119–134, doi: 10.3923/jai.2010.119.134

[36] Thomas, M., Brabanter, K., De Moor, B.: 'New bandwidth selection criterion for kernel PCA: approach to dimensionality reduction and classification problems', *BMC Bioinformatics*, 2014, **15**, p. 137, doi: 10.1186/1471-2105-15-137

[37] Andersen, K., Hansen, L.: 'Model selection for Gaussian kernel PCA denoising', *IEEE Trans. Neural Netw. Learn. Syst.*, 2012, **23**, pp. 163–168, doi: 10.1109/TNNLS.2011.2178325

[38] Nagata, Y., Kado, Y., Onoue, T.*, et al.*: 'Impact of image quality on reliability of the measurements of left ventricular systolic function and global longitudinal strain in 2D echocardiography', *(in Eng), Echo Res. Pract.*, 2018, **5**, (1), pp. 27–39, doi: 10.1530/ERP-17-0047

[39] Queirós, S., Papachristidis, A., Barbosa, D.*, et al.*: 'Aortic valve tract segmentation from 3D-TEE using shape-based B-spline explicit active surfaces', *IEEE Trans. Med. Imaging*, 2016, **35**, pp. 1–1, doi: 10.1109/TMI.2016.2544199